Punjab University Journal of Mathematics (2026), 58(04), 491-517
https://doi.org/10.52280/pujm.2026.58(04)04

Exploring Sombor Indices and Information Entropy of Burbankite Network

Received
14 June, 2026

Revised
07 August, 2026

Accepted
20 August, 2026

Published Online
18 September, 2026

Hafiza Sobia Ishfaq, *Imran Zulfiqar Cheema, Muhammad Kamran Siddiqui
Department of Mathematics,
COMSATS University Islamabad, Lahore Campus, Pakistan

Abstract. Burbankite-type compounds, represented by the chemical formula $(Na, Ca)_3(Sr, Ba, Ce)_3(CO_3)_5$, are distinctive carbonate minerals characterized by the incorporation of alkaline-earth and rare-earth elements, particularly strontium, barium, and cerium. Their are optimal choices for examining the connection between molecular structure and quantitative graph-theoretical descriptions because of their intricate chemical composition and structural arrangement. In this work, the Burbankite-type network's molecular structure is represented by an underlying graph, and its structural properties are quantified using a number of degree-based topological indices. Shannon's information entropy measures, which are derived from degree-based topological indices, are computed to further characterise the network's structural complexity. These entropy metrics offer a numerical evaluation of the network's structural information distribution. In order to investigate the relationship between the studied Sombor-based topological indices and the related information entropies, numerical evaluations and graphical representations are added to the obtained analytical results. The suggested framework may aid in the establishment of quantitative structure–property connections for materials comprising rare-earth and alkaline-earth elements and offers a methodical graph-theoretical approach for characterising complex mineral structures.

AMS (MOS) Subject Classification Codes: 05C09, 05C90, 92E10.
Key Words: Topological Indices; Burbankite Type Network; Entropy.

1. Introduction

There are alternative names for topological indices, such as graph parameters based on vertex degree. Mathematicians and chemists are interested to this study subject as well because of the transdisciplinary implications of topological indices. Since H. Wiener proposed the Wiener index in 1947, almost $3,000$ topological indexes have been implemented in the chemical database.
The Sombor index originally appeared in [10], adopting a geometric interpretation approach. Due to its geometrical problems, these indices has been thoroughly investigated

**Corresponding Author* :imran.cheema@hotmail.com

[14, 15]. Other degree-based vertex attributes have not been proposed from a geometrical perspective. Numerical descriptors derived from the Molecular structure of a substance known as topological indices. They provide information about the structure and interconnectivity of atoms within molecules, which makes them widely used in multiple fields of chemistry and pharmaceutical research [1, 17]. Milan Randic´ initially described a class of topological indices known as the Sombor indices. Drawing from a graph-theoretical approach, they provide details on the molecular structure and properties. Some of the physicochemical properties of molecules that have been predicted by the Sombor indices are boiling temperatures, refractivity, and toxicity [18, 33].

When the Sombor graph parameter emerged in [2021], academics were drawn to it promptly. There is not much literature on this specific index. This Sombor index [29] is literature-based, utilising monogenic semigroup graphs and specific graph procedures. For analysing the Zagreb graph indices, the Sombor graph parameter is used. Also examined in are a few external graph attributes. The Sombor index, in particular, is related to molecular (atomic) orbitals in [16] for topological influence. For a few generalised groups of graphs, generated the sharp constraints on the Sombor graph parameters under discussion in [19].

The bibliometric evaluation of the keywords connected to the Sombor indices that we conducted is shown in Figure 1.

The Sombor index was employed by the researchers in [28] to identify the graphs' exter-

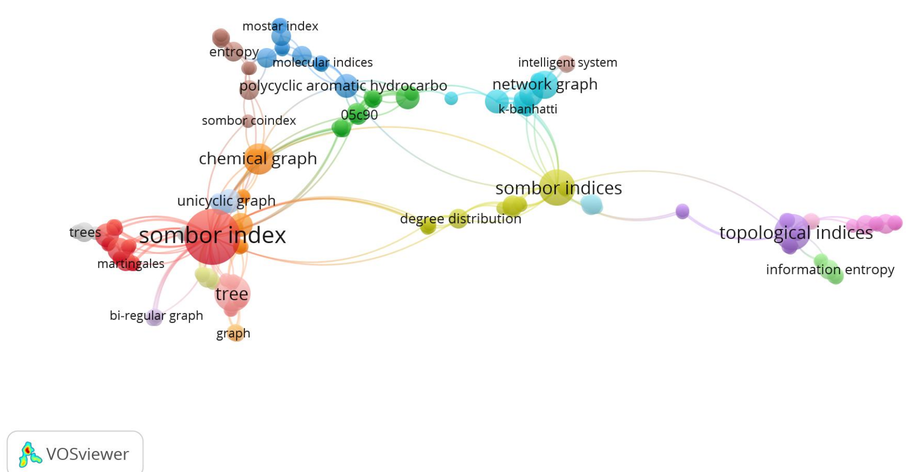

FIGURE 1. Applying bibliometrics to analyze the frequency (Sombor index) of a keyword across published works.

nal constraints. A class of graphs was established, which was external. Using the Sombor index from [30], the author generated the Zagreb indices. The Sombor index and its invariants also provide certain upper and lower bounds. The simplicial networks in [35] are analysed using degree-related parameters and the Sombor index. See [26] for additional information on benzeoid hydrocarbons, their boiling temperatures, and how to apply them in the Sombor graph parameters method. According to their critique of [4], polymers developed dendrimers, according to in the claim [3]. Phenylene chains, hexagonal chains, and the values of the corresponding Sombor index were measured in [12]. Throughout [23], the distinctive features of molecular graphs, the Sombor index, and how they exploit other topological indices are explored. Researchers derived the hypothesis, the Sombor graph parameter, and its invariants in the indicated [11]. Read the specified reference in [13, 25] to find out more about the Sombor index and its outcome. Found [21] to have the most recent findings on Sombor graph parameters and versions.

In chemical graph theory, reverse degree-based topological indices have become a significant class of molecular descriptors. The idea is based on substituting a vertex's (v) reverse degree for its conventional degree $(d(v))$, generally defined as $(d_R(v) = \Delta(G) - d(v) + 1)$, , where $(\Delta(G))$ is the highest vertex degree that (G) has. In order to assess the physico-chemical characteristics of chemical and medicinal substances, reverse Zagreb indices and their variations have been studied. This has shown that reverse-degree descriptors are applicable in molecular structure–property interactions [31].

In order to study reduced reverse Zagreb, hyper-Zagreb, forgotten, atom-bond connectivity, and geometric-arithmetic indices, reverse degree-based indices were subsequently constructed for various molecular and nanostructured networks, such as graphyne and graphdiyne structures [42]. Moreover, iron telluride networks have been subjected to reverse degree-based topological indices, proving their use for statistical analysis and structural characterisation [41]. In order to analyse antiviral medications, reversed degree-based graph invariants have most recently been combined with nonlinear machine-learning models. This shows that reverse degree-based descriptors can function as molecular predictors in contemporary QSPR and machine-learning frameworks[38].

Shannon first introduced the concept of information entropy in his [36] communication theory. It was later discovered that information entropy has wider uses, especially in the context of molecular graphs [7, 22]. Information entropy has two primary uses in chemistry. First, it can be used as a structural descriptor for assessing the sophistication of chemical structures. This application is helpful in categorised both natural and synthetic chemicals Castellano and Torrens [9], setting up a numerical separation of isomers of organic molecules Bonchev, Mekenyan, and Trinajsti [6], and connecting structural and physical and chemical parameters Bonchev and Trinajsti [5]. Second, modelling information transmission and examining physical processes benefit greatly from an understanding of information entropy. While Zhdanov employed entropy values to analyse chemical reactions involving organic molecules, Kobozev emphasised their usefulness in researching these processes Zhdanov [43].

$$ENT_{\xi}(G) = -\sum_{\gamma\Gamma \in E(G)} \frac{\xi(\gamma\Gamma)}{\sum_{\gamma\Gamma \in E(G)} \xi(\gamma\Gamma)} \log\left[\frac{\xi(\gamma\Gamma)}{\sum_{\gamma\Gamma \in E(G)} \xi(\gamma\Gamma)}\right] \tag{1. 1}$$

We assume that the logarithm is in base e for the purposes of this discussion. The variable $\xi(\gamma\Gamma)$ shows the edge set in a graph G. Prior studies have measured an array of graph entropies employing graph order, vertex degrees, and characteristic polynomials. Graph entropies obtained from independent sets, matchings, and vertex degrees have been the focus of more recent work [27]. Several relationships between network complexity and Hosoya entropy were shown by [8]. Additional references for additional research and analysis are [37, 39]. For more information see in [2, 20, 34].

2. Sombor Indices and Their Corresponding Entropy Measures

Assume that G is a simple, nontrivial, correlated graph. Its vertices and edges are designated by the sets $V(G)$ and $E(G)$. An irregular graph is one in which there are discrepancies in the degrees of each vertex; a regular graph has no such discrepancies. The Sombor graph parameter is defined by adding this work on all edges in [40].

$$SO(G) = \sum_{\gamma\Gamma \in E(G)} \sqrt{d_\gamma^2 + d_\Gamma^2} \tag{2. 2}$$

$$SO_{red}(G) = \sum_{\gamma,\Gamma \in E(G)} \sqrt{(d_\gamma - 1)^2 + (d_\Gamma - 1)^2} \tag{2. 3}$$

Simple networks, or graphs without numerous boundaries or loops, are the subject of our attention. The following is a definition of the first and second Zagreb indices:

$$M_1(G) = \sum_{\gamma,\Gamma \in E(G)} [d_\gamma + d_\Gamma] \tag{2. 4}$$

$$M_2(G) = \sum_{\gamma,\Gamma \in E(G)} [d_\gamma \times d_\Gamma] \tag{2. 5}$$

In 1975, Milan Randic derived the first degree topological descriptor: His descriptor was stated as:

$$R(G) = \sum_{\gamma,\Gamma \in E(G)} \frac{1}{\sqrt{d_\gamma \times d_\Gamma}} \tag{2. 6}$$

In 1987 , Faijtlowicz defined the Harmonic indicator and stated as:

$$H(G) = \sum_{\gamma,\Gamma \in E(G)} \frac{2}{d_\gamma + d_\Gamma} \tag{2. 7}$$

Let $d_G(e)$ represent the degree of an arc $e \in G$, which is represented by $d_G(e) = d_G(\gamma) + d_G(\Gamma) - 2$ with $e = \gamma\Gamma$. The first and second K Banhatti descriptors [24] are stated as:

$$\beta_1(G) = \sum_{\gamma,\Gamma \in E(G)} d_{\gamma\Gamma} + d(e) \tag{2. 8}$$

$$\beta_2(G) = \sum_{\gamma,\Gamma \in E(G)} d_{\gamma\Gamma} \times d(e) \tag{2. 9}$$

- **Sombor Entropy**

By substituting the values from equation 1.1 into equation 2.2 and simplifying, the resulting expression is:

$$ENT_{SO}(G) = \log(SO(G)) - \frac{1}{(SO(G))} \log \left[\sum_{\gamma\Gamma \in E(G)} \sqrt{d_\gamma^2 + d_\Gamma^2}^{\sum_{\gamma\Gamma \in E(G)} \sqrt{d_\gamma^2 + d_\Gamma^2}} \right] \tag{2. 10}$$

- **Sombor Reduced Entropy**

By substituting the values from equation 1.1 into equation 2.3 and simplifying, the resulting expression is:

$$\begin{aligned} ENT_{SO_{red}}(G) = {} & \log\left(SO_{red}(G)\right) \\ & - \frac{1}{SO_{red}(G)} \log \left[\sum_{\gamma,\Gamma \in E(G)} \sqrt{(d_\gamma - 1)^2 + (d_\Gamma - 1)^2}^{\sum_{\gamma,\Gamma \in E(G)} \sqrt{(d_\gamma - 1)^2 + (d_\Gamma - 1)^2}} \right]. \end{aligned} \tag{2. 11}$$

- **First Zagreb Entropy**

By substituting the values from equation 1.1 into equation 2.4 and simplifying, the resulting expression is:

$$\begin{aligned} ENT_{M_1}(G) = {} & \log\left(M_1(G)\right) \\ & - \frac{1}{M_1(G)} \log \left[\sum_{\gamma,\Gamma \in E(G)} \sqrt{(d_\gamma - 1)^2 + (d_\Gamma - 1)^2}^{\sum_{\gamma,\Gamma \in E(G)} \sqrt{(d_\gamma - 1)^2 + (d_\Gamma - 1)^2}} \right]. \end{aligned} \tag{2. 12}$$

- **Second Zagreb Entropy**

By substituting the values from equation 1.1 into equation 2.5 and simplifying, the resulting expression is:

$$ENT_{M_2}(G) = \log(M_2(G)) - \frac{1}{M_2(G)} \log \left[\sum_{\gamma,\Gamma \in E(G)} [d_\gamma \times d_\Gamma]^{\sum_{\gamma,\Gamma \in E(G)} [d_\gamma \times d_\Gamma]} \right] \tag{2. 13}$$

- **Randic Entropy**

By substituting the values from equation 1.1 into equation 2.6 and simplifying, the resulting expression is:

$$ENT_R(G) = \log(R(G)) - \frac{1}{R(G)} \log \left[\sum_{\gamma,\Gamma \in E(G)} \frac{1}{\sqrt{d_\gamma \times d_\Gamma}}^{\sum_{\gamma,\Gamma \in E(G)} \frac{1}{\sqrt{d_\gamma \times d_\Gamma}}} \right] \tag{2. 14}$$

- **Harmonic Entropy**

By substituting the values from equation 1.1 into equation 2.7 and simplifying, the resulting expression is:

$$ENT_H(G) = \log(H(G)) - \frac{1}{H(G)} \log \left[\sum_{\gamma,\Gamma \in E(G)} \frac{2}{d_\gamma + d_\Gamma}^{\sum_{\gamma,\Gamma \in E(G)} \frac{2}{d_\gamma + d_\Gamma}} \right] \tag{2. 15}$$

- **First K Banhatti Entropy**

By substituting the values from equation 1.1 into equation 2.8 and simplifying, the resulting expression is:

$$ENT_{\beta_1}(G) = \log(\beta_1(G)) - \frac{1}{\beta_1(G)} \log \left[\sum_{\gamma,\Gamma \in E(G)} d_{\gamma\Gamma} + d(e)^{\sum_{\gamma,\Gamma \in E(G)} d_{\gamma\Gamma} + d(e)} \right] \tag{2. 16}$$

- **Second K Banhatti Entropy**

By substituting the values from equation 1.1 into equation 2.9 and simplifying, the resulting expression is:

$$ENT_{\beta_2}(G) = \log(\beta_2(G)) - \frac{1}{\beta_2(G)} \log \left[\sum_{\gamma,\Gamma \in E(G)} d_{\gamma\Gamma} \times d(e)^{\sum_{\gamma,\Gamma \in E(G)} d_{\gamma\Gamma} \times d(e)} \right] \tag{2. 17}$$

3. The Structure of Burbankite Network

Burbankite-type structures are composed of connected points or nodes that exhibit a specific form of symmetry. This pattern is distinguished by a set of connected subgraphs that share vertices and nodes. These subgraphs form a framework that resembles a tree, with the centre node acting as the hub connecting all other nodes within the group. The burbankite-type structure is a crystallographic arrangement that indicates a particular arrangement of atoms or ions within a crystal lattice. An array of polygonal or polyhedral components that interpenetrate one another is frequently used in this structure. As its name implies, burbankite is a calcium carbonate mineral that was discovered in the San Gabriel Mountains in Burbank, California. Burbankite-type structures are of particular interest to researchers in the fields of solid-state chemistry, material sciences, and crystallography due to their unique interpenetrating layers, chiral ordering, and polygonal or polyhedral units [32].

Burbankite-type structures can be used to indicate the composition and structure of other minerals and crystalline materials. The structure-property correlations in these systems can be enhanced by examining the physical and chemical properties of these materials. A mineral sample may be recognised and categorised more easily if it has Burbankite-type structures, especially if the arrangement of the units and their linkages to other units in the lattice are peculiar or unusual. Burbankite-type formation examination can provide valuable insights into the properties and morphologies of an assortment of materials, such as metals, semiconductors, and dielectrics. This information can be used to create new materials with the needed qualities, enhance existing materials, or establish more efficient manufacturing processes. Carbon nanotubes, supramolecular assemblies, protein crystal structures, and other molecular systems can all be modelled and constructed using Burbankite-type structures. The reason for this is the way the units are built and arranged in these structures. The Burabnkite-type structure is shown in figure 2. The degree-based vertex and edge partition is shown in table 1 and table 2 respectively.

TABLE 1. Degree-based Vertex partition

(d_γ)	Frequency	Edge Vertex Set
2	$(3(r+s)+1)$	V_1
3	$(2r+2s-4)$	V_2
4	$(6rs-4r-4s+3)$	V_3

TABLE 2. Degree-based Edge partition

(d_γ, d_Γ)	Frequency	Edge Set
$(2,2)$	5	E_1
$(2,3)$	$(2r+2s-4)$	E_2
$(2,4)$	$(4r+4s-4)$	E_3
$(3,3)$	$(r+s-2)$	E_4
$(3,4)$	$(2r+2s-4)$	E_5
$(4,4)$	$(12rs-11r-11s+10)$	E_6

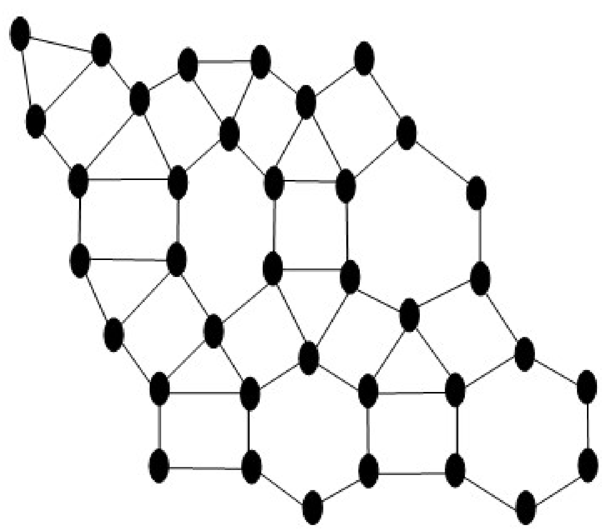

FIGURE 2. Burbankite-type structure

- The $SO(G)$ index of Burbankite-type network

$$
\begin{aligned}
SO(G) &= \sum_{\gamma\Gamma\in E(G)} \sqrt{d_\gamma^2+d_\Gamma^2} \\
&= \sqrt{2^2+2^2}(5)+\sqrt{2^2+3^2}(2r+2s-4)+\sqrt{2^2+4^2}(4r+4s-4) \\
&+ \sqrt{3^2+3^2}(r+s-2)+\sqrt{3^2+4^2}(2r+2s-4) \\
&+ \sqrt{4^2+4^2}(12rs-11r-11s+10) \\
&= 67.8rs-22.83r-22.83s-9.88
\end{aligned}
$$

- The $SO_{red}(G)$ index of Burbankite-type network

$$
\begin{aligned}
SO_{red}(G) = &\sum_{\gamma,\Gamma\in E(G)} \sqrt{(d_\gamma-1)^2+(d_\Gamma-1)^2} \\
&= \sqrt{(2-1)^2+(2-1)^2}(5) \\
&\quad+ \sqrt{(2-1)^2+(3-1)^2}(2r+2s-4) \\
&\quad+ \sqrt{(2-1)^2+(4-1)^2}(4r+4s-4) \\
&\quad+ \sqrt{(3-1)^2+(3-1)^2}(r+s-2) \\
&\quad+ \sqrt{(3-1)^2+(4-1)^2}(2r+2s-4) \\
&\quad+ \sqrt{(4-1)^2+(4-1)^2}(12rs-11r-11s+10) \\
&= 50.88rs-19.52r-19.52s+7.87.
\end{aligned}
$$

- The $M_1(G)$ index of Burbankite-type network

$$
\begin{aligned}
M_1(G) &= \sum_{\gamma,\Gamma\in E(G)} [d_\gamma+d_\Gamma] \\
&= (2+2)(5)+(2+3)(2r+2s-4)+(2+4)(4r+4s-r) \\
&+ +(3+3)(r+s-2)(3+4)(2r+2s-4)[2mm] \\
&+ +(4+4)(12rs-11r-11s+10) \\
&= 96rs-34r-34s+16
\end{aligned}
$$

- The $M_2(G)$ index of Burbankite-type network

$$\begin{aligned}
M_2(G) &= \sum_{\gamma,\Gamma\in E(G)} [d_\gamma \times d_\Gamma] \\
&= 4(5) + 6(2r+2s-4) + 8(4r+4s-4) + 9(r+s-2) + 12(24+2s-4) \\
&+ 16(12rs-11r-11s+10) \\
&= 192rs - 99r - 99s + 58
\end{aligned}$$

- The $R(G)$ index of Burbankite-type network

$$\begin{aligned}
R(G) &= \sum_{\gamma,\Gamma\in E(G)} \frac{1}{\sqrt{d_\gamma \times d_\Gamma}} \\
&= \frac{5}{\sqrt{4}} + \frac{(2r+2s-4)}{\sqrt{6}} + \frac{(4r+4s-4)}{\sqrt{8}} + \frac{(r+s-2)}{\sqrt{9}} \\
&+ \frac{(2r+2s-4)}{\sqrt{12}} + \frac{(12rs-11r-11s+10)}{\sqrt{16}} \\
&= 3rs + 0.3915r + 0.3915s + 0.1314
\end{aligned}$$

- The $H(G)$ index of Burbankite-type network

$$\begin{aligned}
H(G) = &\sum_{\gamma,\Gamma\in E(G)} \frac{2}{d_\gamma + d_\Gamma} \\
= &\left(\frac{2}{2+2}\right)(5) + \left(\frac{2}{2+3}\right)(2r+2s-4) \\
&+ \left(\frac{2}{2+4}\right)(4r+4s-4) + \left(\frac{2}{3+3}\right)(r+s-2) \\
&+ \left(\frac{2}{3+4}\right)(2r+2s-4) \\
&+ \left(\frac{2}{4+4}\right)(12rs-11r-11s+10) \\
= &\, 3rs + \frac{121}{420}r + \frac{121}{420}s + \frac{9}{35}.
\end{aligned}$$

- The $\beta_1(G)$ index of Burbankite-type network

$$\begin{aligned}
\beta_1(G) = &\sum[d_\gamma + d(e)] \\
&= [(2+2)+(2+2)](5) \\
&\quad + [(2+3)+(3+3)](2r+2s-4) \\
&\quad + [(2+4)+(4+2)](4r+4s-4) \\
&\quad + [(3+4)+(3+4)](r+s-2) \\
&\quad + [(3+5)+(4+5)](2r+2s-4) \\
&\quad + [(4+6)+(4+6)](12rs-11r-11s+10) \\
&= 240rs - 102r - 102s + 52.
\end{aligned}$$

- The $\beta_2(G)$ index of Burbankite-type network

$$\begin{aligned}
\beta_2(G) = &\sum[d_\gamma \times d(e)] \\
&= [(2+2)(2+2)](5) \\
&\quad + [(2+3)(3+3)](2r+2s-4) \\
&\quad + [(2+4)(4+2)](4r+4s-4) \\
&\quad + [(3+4)(3+4)](r+s-2) \\
&\quad + [(3+5)(4+5)](2r+2s-4) \\
&\quad + [(4+6)(4+6)](12rs-11r-11s+10) \\
&= 1200rs - 703r - 703s + 430.
\end{aligned}$$

3.1. **Graphical and Numerical Comparison.** A numerical comparison across multiple graph invariants for various values of the parameters r and s is shown in the table 3. All of the indices and descriptors have rises in concert with r and s. This exhibits a positive correlation between the topological indices and the graph's size or the values of r and s, implying that as r and s rises, the graph's complexity or connectivity may also increase. For all values of r and s, the sombor index $SO(G)$ is substantially greater than the reduced sombor index $SO_{red}(G)$, also shown graphically in figure 3. Since $M_1(G)$ is typically larger but near $M_2(G)$ as shown in figure 4, it indicates that the degree-based structure is symmetric.

The Zagreb indices are helpful for analysing vertex degree contributions. With higher values of r and s, both the harmonic index $H(G)$ and the Randic index $R(G)$ demonstrate similar patterns of continual rise which is also presented in figure 5. Because they employ distinct techniques to capture graph structure, the harmonic index has a tendency to be marginally larger than the Randic index. As r and s increase, there is a noticeable increase in both $\beta_1(G)$ and $\beta_2(G)$ as presented graphically in figure 6. Specifically, $\beta_2(G)$ increases significantly more quickly than $\beta_1(G)$, suggesting that when the graph's size or degree increases, the second descriptor captures greater or more complicated structures in the graph. As an illustration, $\beta_2(G)$ approaches 106370, whereas the sombor index $SO(G)$ rises to 6313.52. This indicates that these indices have an exponential or extremely non-linear growth, indicating that as the parameters increase, the underlying graph structure gets more complex.

TABLE 3. Numerical comparison of $SO(G)$, $SO_{red}(G), M_1(G), M_2(G), R(G), H(G), \beta_1(G), \beta_2(G)$

(r,s)	$SO(G)$	$SO_{red}(G)$	$M_1(G)$	$M_2(G)$	$R(G)$	$H(G)$	$\beta_1(G)$	$\beta_2(G)$
$(1,1)$	$12,26$	19.7100	44	52	3.9144	3.8333	88	224
$(2,2)$	170.0000	133.3100	264	430	13.6974	13.4095	604	2418
$(3,3)$	463.3400	348.6700	676	1192	29.4804	28.9857	1600	7012
$(4,4)$	892.2800	665.7900	1280	2338	51.2634	50.5619	3076	14006
$(5,5)$	1456.8200	14.6700	2076	3868	79.0464	78.1381	5032	2340
$(6,6)$	2156.9600	1605.3100	3064	5782	112.8294	111.7143	7468	35194
$(7,7)$	2992.70000	2227.7100	4244	8080	152.6124	151.2905	10384	49388
$(8,8)$	3964.0400	2951.8700	5616	10762	198.3954	196.8667	13780	65982
$(9,9)$	5070.9800	3777.7900	7180	13828	250.1782	248.4429	17656	84976
$(10,10)$	6313.5200	4705.4700	8936	17278	307.9614	306.0191	22012	106370

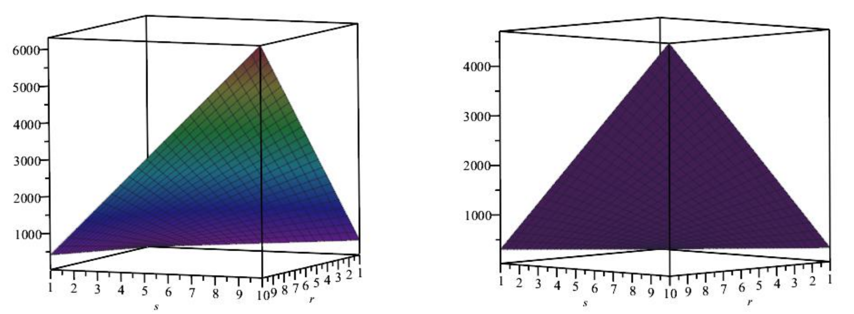

(A) (B)

FIGURE 3. (a) Sombor index (b) Reduced Sombor index

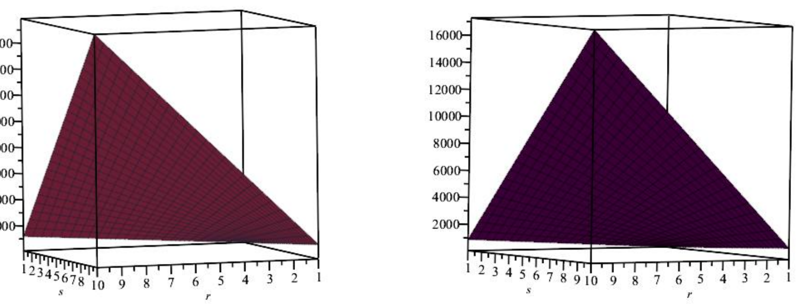

(A) (B)

FIGURE 4. (a)First Zagreb index (b) Second Zagreb index

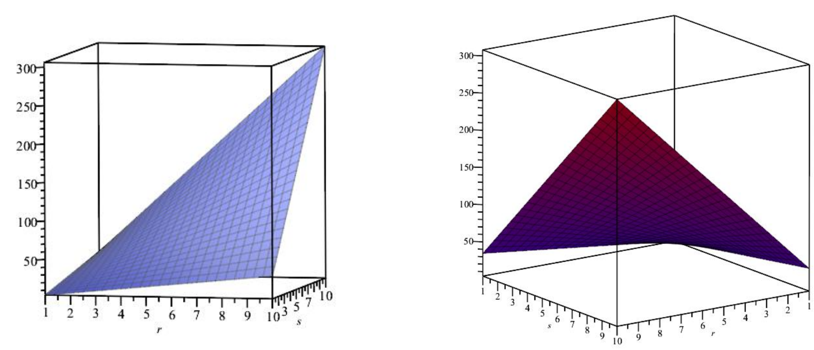

(A) (B)

FIGURE 5. (a) Harmonic index (b) Randic index

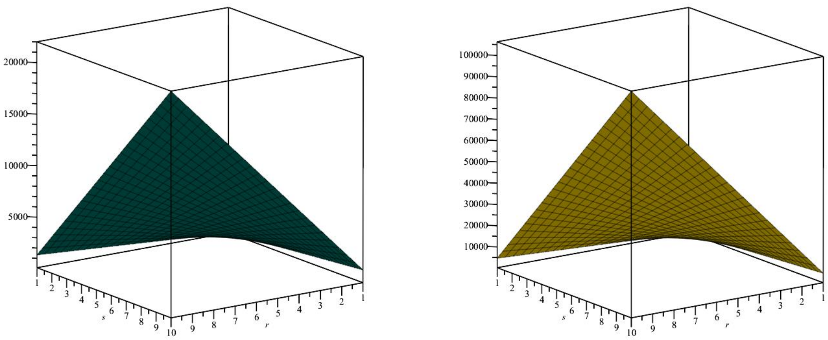

(A) (B)

FIGURE 6. (a) First K Banhatti index (b) Second K Banhatti index

The main objective of our work is to compute the entropy measure using various topological indices. This method enables us to quantify the complexity or information content of a system based on its topological properties. The entropy measures is computed below for the above calculated indices.

- **Sombor Entropy of Burbankite-type network**

By utilizing the data from table 2 and equation 2.10, we can derive the following results:

$$\begin{aligned} ENT_{SO}(G) = {} & \log(67.8rs - 22.83r - 22.83s - 9.88) \\ & - \frac{5\log\left(\sqrt{8}\right)^{\sqrt{8}}}{67.8rs - 22.83r - 22.83s - 9.88} \\ & - \frac{(2r+2s-4)\log\left(\sqrt{13}\right)^{\sqrt{13}}}{67.8rs - 22.83r - 22.83s - 9.88} \\ & - \frac{(4r+4s-4)\log\left(\sqrt{20}\right)^{\sqrt{20}}}{67.8rs - 22.83r - 22.83s - 9.88} \\ & - \frac{(r+s-2)\log\left(\sqrt{18}\right)^{\sqrt{18}}}{67.8rs - 22.83r - 22.83s - 9.88} \\ & - \frac{(2r+2s-4)\log(5)^{5}}{67.8rs - 22.83r - 22.83s - 9.88} \\ & - \frac{(12rs - 11r - 11s + 10)\log\left(\sqrt{32}\right)^{\sqrt{32}}}{67.8rs - 22.83r - 22.83s - 9.88}. \end{aligned}$$

- **Reduced Sombor Entropy of Burbankite-type network**

By utilizing the data from table 2 and equation 2.11, we can derive the following results:

$$
\begin{aligned}
ENT_{SO_{red}}(G) = & \log(50.88rs - 19.52r - 19.52s + 7.87) \\
& - \frac{5\log\left(\sqrt{2}\right)^{\sqrt{2}}}{50.88rs - 19.52r - 19.52s + 7.87} \\
& - \frac{(2r + 2s - 4)\log\left(\sqrt{5}\right)^{\sqrt{5}}}{50.88rs - 19.52r - 19.52s + 7.87} \\
& - \frac{(4r + 4s - 4)\log\left(\sqrt{10}\right)^{\sqrt{10}}}{50.88rs - 19.52r - 19.52s + 7.87} \\
& - \frac{(r + s - 2)\log\left(\sqrt{8}\right)^{\sqrt{8}}}{50.88rs - 19.52r - 19.52s + 7.87} \\
& - \frac{(2r + 2s - 4)\log\left(\sqrt{13}\right)^{\sqrt{13}}}{50.88rs - 19.52r - 19.52s + 7.87} \\
& - \frac{(12rs - 11r - 11s + 10)\log\left(\sqrt{18}\right)^{\sqrt{18}}}{50.88rs - 19.52r - 19.52s + 7.87}.
\end{aligned}
$$

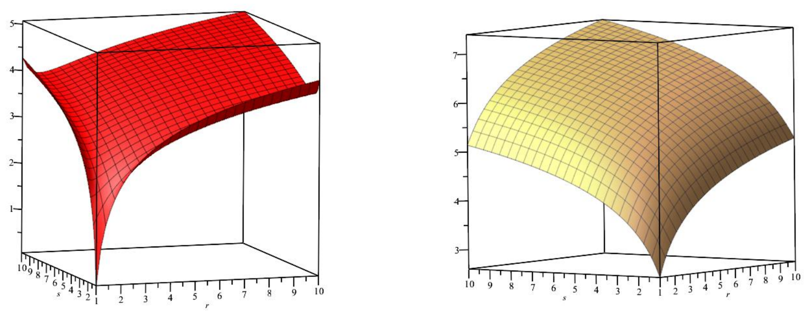

(A) (B)

FIGURE 7. (a) Sombor Entropy (b) Reduced Sombor Entropy

The $ENT_{SO}(G)$ is consistently smaller than $ENT_{SO_{red(G)}}$ across all values of r and s. This inversion implies that the reduced index makes a greater contribution to information theory through the entropy reduction process, presumably as a result of $SO_{red(G)}$ more compact structural representation also shown graphically in figure 7.

- **First Zagreb Entropy of Burbankite-type network**

By utilizing the data from table 2 and equation 2.12, we can derive the following results:

$$\begin{aligned} ENT_{M_1}(G) &= \log(96rs-34r-34s+16) - \frac{(5)\log(4)^4}{(96rs-34r-34s+16)} \\ &- \frac{(2r+2s-4)\log(5)^5}{(96rs-34r-34s+16)} - \frac{(4r+4s-4)\log(6)^6}{(96rs-34r-34s+16)} \\ &- \frac{(r+s-2)\log(6)^6}{(96rs-34r-34s+16)} - \frac{(2r+2s-4)\log(7)^7}{(96rs-34r-34s+16)} \\ &- \frac{(12rs-11r-11s+10)\log(8)^8}{(96rs-34r-34s+16)}. \end{aligned}$$

- **Second Zagreb Entropy of Burbankite-type network**

By utilizing the data from table 2 and equation 2.13, we can derive the following results:

$$\begin{aligned} ENT_{M_2}(G) &= \log(192rs-99r-99s+58) - \frac{(5)\log(4)^4}{(192rs-99r-99s+58)} \\ &- \frac{(2r+2s-4)\log(6)^6}{(192rs-99r-99s+58)} - \frac{(4r+4s-4)\log(8)^8}{(192rs-99r-99s+58)} \\ &- \frac{(r+s-2)\log(9)^9}{(192rs-99r-99s+58)} - \frac{(2r+2s-4)\log(12)^{12}}{(192rs-99r-99s+58)} \\ &- \frac{(12rs-11r-11s+10)\log(16)^{16}}{(192rs-99r-99s+58)}. \end{aligned}$$

As a more prominent measure of the entire vertex degree distribution, the first Zagreb index consistently displays more of a contribution from the vertex degrees in terms of entropy as shown in figure 8.

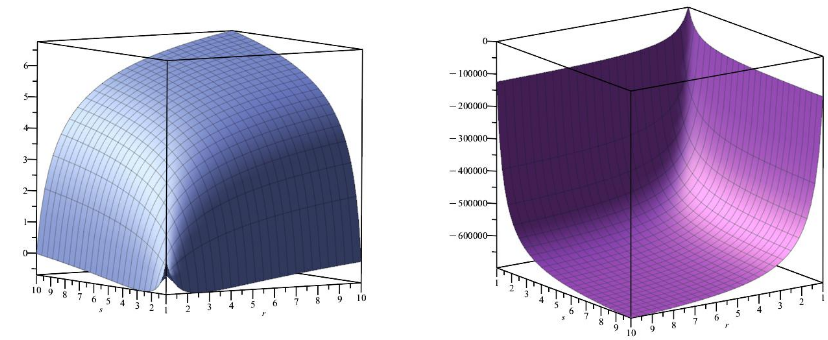

(A) (B)

FIGURE 8. (a) First Zagreb Entropy (b) Second Zagreb Entropy

- **Randic Entropy of Burbankite-type network**

By utilizing the data from table 2 and equation 2.14, we can derive the following results:

$$\begin{aligned}
ENT_R(G) = \ & \log(3rs + 0.3915r + 0.3915s + 0.1314) \\
& - \frac{5\log\left(\frac{1}{2}\right)^{\frac{1}{2}}}{3rs + 0.3915r + 0.3915s + 0.1314} \\
& - \frac{(2r + 2s - 4)\log\left(\frac{1}{\sqrt{6}}\right)^{\frac{1}{\sqrt{6}}}}{3rs + 0.3915r + 0.3915s + 0.1314} \\
& - \frac{(4r + 4s - 4)\log\left(\frac{1}{\sqrt{8}}\right)^{\frac{1}{\sqrt{8}}}}{3rs + 0.3915r + 0.3915s + 0.1314} \\
& - \frac{(r + s - 2)\log\left(\frac{1}{3}\right)^{\frac{1}{3}}}{3rs + 0.3915r + 0.3915s + 0.1314} \\
& - \frac{(2r + 2s - 4)\log\left(\frac{1}{\sqrt{12}}\right)^{\frac{1}{\sqrt{12}}}}{3rs + 0.3915r + 0.3915s + 0.1314} \\
& - \frac{(12rs - 11r - 11s + 10)\log\left(\frac{1}{4}\right)^{\frac{1}{4}}}{3rs + 0.3915r + 0.3915s + 0.1314}.
\end{aligned}$$

- **Harmonic Entropy of Burbankite-type network**

By utilizing the data from table 2 and equation 2.15, we can derive the following results:

$$\begin{aligned} ENT_H(G) &= \log\left(3rs+\frac{121}{420}r+\frac{121}{420}s+\frac{9}{35}\right)-\frac{(5)\log(\frac{1}{2})^{\frac{1}{2}}}{\left(3rs+\frac{121}{420}r+\frac{121}{420}s+\frac{9}{35}\right)} \\ &- \frac{(2r+2s-4)\log(\frac{1}{3})^{\frac{1}{3}}}{\left(3rs+\frac{121}{420}r+\frac{121}{420}s+\frac{9}{35}\right)}-\frac{(4r+4s-4)\log(\frac{1}{4})^{\frac{1}{4}}}{\left(3rs+\frac{121}{420}r+\frac{121}{420}s+\frac{9}{35}\right)} \\ &- \frac{(r+s-2)\log(\frac{2}{9})^{\frac{2}{9}}}{\left(3rs+\frac{121}{420}r+\frac{121}{420}s+\frac{9}{35}\right)}-\frac{(2r+2s-4)\log(\frac{1}{6})^{\frac{1}{6}}}{\left(3rs+\frac{121}{420}r+\frac{121}{420}s+\frac{9}{35}\right)} \\ &- \frac{(12rs-11r-11s+10)\log(\frac{1}{8})^{\frac{1}{8}}}{\left(3rs+\frac{121}{420}r+\frac{121}{420}s+\frac{9}{35}\right)}. \end{aligned}$$

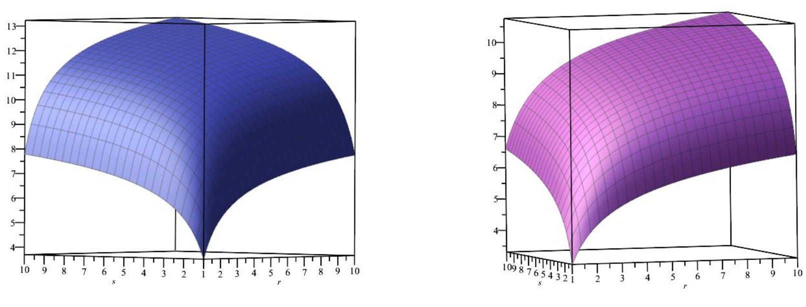

(A) (B)

FIGURE 9. (a) Harmonic Entropy (b) Randic Entropy

With respect to other indices, the harmonic index, $ENT_{H(G)}$, and the entropy-based Randic index, $ENT_{R(G)}$, both exhibit extremely little development which is presented in figure 9.

- **First K banhatti Entropy of Burbankite-type network**

By utilizing the data from table 2 and equation 2.16, we can derive the following results:

$$\begin{aligned}
ENT_{\beta_1}(G) &= \log(240rs-102r-102s+52)-\frac{(5)\log(8)^8}{(240rs-102r-102s+52)}\\
&- \frac{(2r+2s-4)\log(11)^{11}}{(240rs-102r-102s+52)}-\frac{(4r+4s-4)\log(12)^{12}}{(240rs-102r-102s+52)}\\
&- \frac{(r+s-2)\log(14)^{14}}{(240rs-102r-102s+52)}-\frac{(2r+2s-4)\log(17)^{17}}{(240rs-102r-102s+52)}\\
&- \frac{(12rs-11r-11s+10)\log(20)^{20}}{(240rs-102r-102s+52)}.
\end{aligned}$$

- **Second K banhatti Entropy of Burbankite-type network**

By utilizing the data from table 2 and equation 2.17, we can derive the following results:

$$\begin{aligned}
ENT_{\beta_2}(G) &= \log(1200rs-703r-703s+430)-\frac{(5)\log(16)^{16}}{(1200rs-703r-703s+430)}\\
&- \frac{(2r+2s-4)\log(30)^{30}}{(1200rs-703r-703s+430)}-\frac{(4r+4s-4)\log(36)^{36}}{(1200rs-703r-703s+430)}\\
&- \frac{(r+s-2)\log(49)^{49}}{(1200rs-703r-703s+430)}-\frac{(2r+2s-4)\log(72)^{72}}{(1200rs-703r-703s+430)}\\
&- \frac{(12rs-11r-11s+10)\log(100)^{100}}{(1200rs-703r-703s+430)}.
\end{aligned}$$

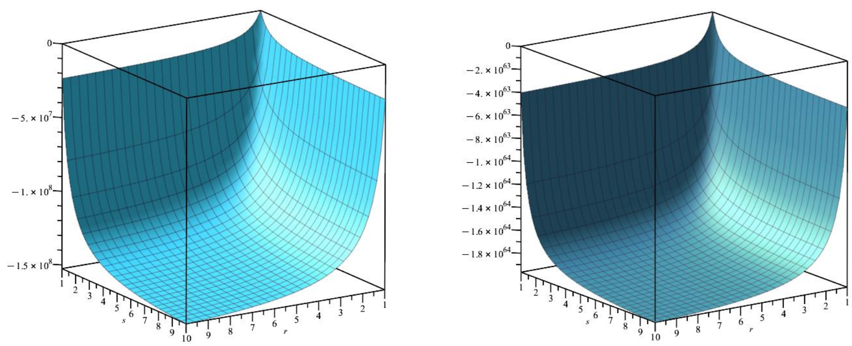

(A) (B)

FIGURE 10. (a) First K Bnahatti Entropy (b) Second K Banhatti Entropy

In comparison to their original forms, the entropy-based topological descriptors $(ENT_{\beta_1(G)}, ENT_{\beta_2(G)})$ still offer an informative picture of the graph's complexity, but it does so in a more controlled manner as presented graphically in figure 10.
In the table 4, entropy-based indices acquired from various graph invariants are numerically

TABLE 4. Numerical comparison of $ENT_{SO(G)}, ENT_{SO_{red}(G)}$, $ENT_{M_1(G)}, ENT_{M_2(G)}, ENT_{R(G)}$, $ENT_{H(G)}, ENT_{\beta_1(G)}, ENT_{\beta_2(G)}$

(r,s)	ENT_{SO}	ENT_{SOred}	ENT_{M1}	ENT_{M2}	ENT_R	ENT_H	ENT_{β_1}	ENT_{β_2}
$(1,1)$	0.06341	2.6074	0.3560	23.297	1.0872	1.3436	2534.7	1.6118
$(2,2)$	2.4588	4.1340	1.2634	397610	1.4350	1.6821	7.8862	1.2233
$(3,3)$	3.0775	4.9667	2.8868	532390	1.3052	1.4215	1.1037	1.5668
$(4,4)$	3.5216	5.5514	3.9547	594930	1.0920	1.1119	1.2576	1.7197
$(5,5)$	3.8799	6.0033	4.7163	630830	0.8699	0.8207	1.3483	1.8059
$(6,6)$	4.1824	6.3712	5.2980	654040	0.6578	0.5583	1.4077	1.8610
$(7,7)$	4.4446	6.6821	5.7642	670310	0.4600	0.3234	1.4498	1.8994
$(8,8)$	4.6761	6.9508	6.1512	682330	0.2764	0.1089	1.4812	1.9277
$(9,9)$	4.8835	7.1879	6.4808	691570	0.1063	0.0854	1.5054	1.9494
$(10,10)$	5.0714	7.3998	6.7672	698880	0.0519	0.2634	1.5246	1.9664

examined for a range of values of r and s. All entropy-based indices rise in tandem with rising values of r and s, similar to in the prior table. On the other hand, compared to the original indices, the development in these entropy measures appears more gradual, demonstrating that the entropic nature of these measurements dampens the growth rate of the graph invariants. This indicates that these two indices, maybe because of their innate ability to capture more nuanced topological features, become less susceptible to changes in the structure and connectivity of the graph when converted into entropy measurements.

4. Rational Curve fitting among indices and their associated information entropy

Rational curve fitting is a method that uses a ratio of two polynomials, usually represented as $f(x) = \frac{P(x)}{(Q)}$ to approximate data points. $P(x)$ and $Q(x)$ are the polynomials in this example. With more flexibility than linear and polynomial fits, this method is useful for capturing complicated, nonlinear relationships in data. It is especially helpful in cases where the data possess poles values of x at which the function tends to infinity, or asymptotic behavior, in which the function approaches a value as x increases.

Entropy, when it pertains to indices and entropy, is an indicator of indeterminacy or disorder in a system that is frequently utilised in statistical mechanics, thermodynamics, and information theory. In a variety of disciplines covering information systems, ecological systems, and economic models, entropy indices are used to measure diversity or volatility. Nonlinear behaviour is frequently seen in the relationship between indices (such diversity or complexity indices) and the accompanying entropy values. An effective way to model these interactions is by rational curve fitting, which picks up on minute differences in the data that polynomial or linear fitting methods might overlook. The link between entropy and indices has been determined via a variety of curve fitting techniques that use numerous parameter versions, including linear, power, polynomial, and rational fitting. We analysed the accuracy using mean squared error (MSE), sum of squared error (SSE) normalized by mean(Nbm), and R^2 with an emphasis on MSE. The most accurate results have been generated in every instance using the rational fitting method. Below are the general models for indices versus entropy.

$$ENT(SO) = \frac{p_1 x + p_2}{x^4 + q_1 x^3 + q_2 x^2 + q_3 x + q_4}$$

where x is Nbm 3349 and standard deviation is 3575. The Coefs with (with 95% confidence bounds) are $p_1 = 9.44e + 04(-7.038e + 07, 7.057e + 07)$, $p_2 = 8.816e + 04(-6.572e + 07, 6.59e + 07)$, $q_1 = 2693(-2.009e + 06, 2.014e + 06)$, $q_2 = -1869(-1.396e + 06, 1.392e + 06)$, $q_3 = 1.612e + 04(-1.202e + 07, 1.205e + 07)$, $q_4 = 1.944e + 04(-1.45e + 07, 1.453e + 07)$

$$ENT(SO_{red}) = \frac{p_1 x^2 + p_2 x + p_3}{x^5 + q_1 x^4 + q_2 x^3 + q_3 x^2 + q_4 x + q_5}$$

where x is Nbm 1752 and standard deviation is 1624. The Coefs (with 95% confidence bounds) are $p_1 = 4.131e + 04(-2.782e + 07, 2.791e + 07)$, $p_2 = 1.307e + 05(-8.754e + 07, 8.78e + 07)$, $p_3 = 9.368e + 04(-6.255e + 07, 6.273e + 07)$, $q_1 = -45.8(-2.895e + 04, 2.886e+04)$, $q_2 = 12.54(-6756, 6781)$, $q_3 = 4829(-3.256e+06, 3.265e+06)$, $q_4 =$

$1.823e+04(-1.222e+07, 1.225e+07)$, $q_5 = 1.451e+04(-9.686e+06, 9.715e+06)$.

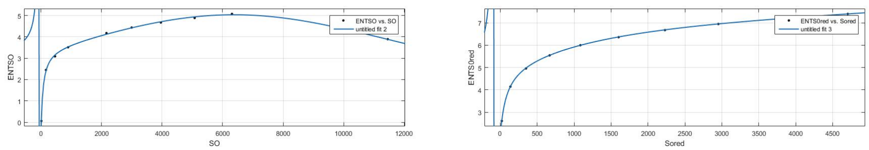

(A) (B)

FIGURE 11. (a) Sombor index vs Entropy (b) Reduced Sombor index vs Entropy

TABLE 5. Integrity of fit for entropy vs SO, SO_{red} indices of Burbankite-type network

Indices	Fit-type	SSE	R^2	$RMSE$
$ENT(SO)$	$r14$	0.01607	0.9982	0.06338
$ENT(SO_{red})$	$r25$	0.0003425	0.9999	0.01309

The Numerical Integrity of fit for entropy vs indices of Burbankite-type network are depicted in table 5. The figure 11 shows how, when entropy rises, the sombor index first rises quickly before progressively approaching a maximum. The graph indicates a rise that is logarithmic in nature, with the sombor index growing significantly in the early phases of increasing entropy before beginning to level off. The initial steep spike indicates the speed at which the sombor index adjusts to entropy changes in smaller or simpler graphs. The plot of the reduced sombor index $SO_{red(G)}$ versus entropy shows a similar trend to the sombor index, but it remains at lower values overall. This curve depicts how the reduced sombor index becomes more sensitive at lower entropy levels before plateauing as entropy rises, revealing the structural details lost during the reduction process.

$$ENT(M_1) = \frac{p_1x + p_2}{x^4 + q_1x^3 + q_2x^2 + q_3x + q_4}$$

where x is Nbm 3338 and standard deviation is 3080. The Coefs (with 95% confidence bounds) are $p_1 = 226.1(-348.5, 800.7)$, $p_2 = 245.6(-376.8, 868.1)$,
$q_1 = -1.759(-3.694, 0.1756)$, $q_2 = -1.908(-5.037, 1.22)$, $q_3 = 31.81(-46.77, 110.4)$,
$q_4 = 45.3(-68.8, 159.4)$

$$ENT(M_2) = \frac{p_1x^4 + p_2x^3 + p_3x^2 + p_4x + p_5}{x^4 + q_1x^3 + q_2x^2 + q_3x + q_4}$$

The Coefs (with 95% confidence bounds) are $p_1 = 7.112e+05(-1.594e+06, 3.017e+06)$, $p_2 = -4.384e+07(-5.223e+23, 5.223e+23)$, $p_3 = -1.028e+06(-3.171e+25, 3.171e+25)$, $p_4 = -1.899e+04(-3.034e+25, 3.034e+25)$, $p_5 = -358.2(-2.798e+25, 2.798e+25)$, $q_1 = 405.6(-7.344e+17, 7.344e+17)$, $q_2 = -8.206e+04(-2.986e+$

$20, 2.986e + 20)$, $q_3 = 2.273e + 06(-5.999e + 22, 5.999e + 22)$, $q_4 = -2.051e + 06(-1.614e + 24, 1.614e + 24)$.

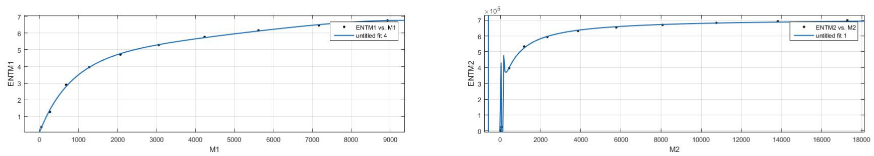

(A) (B)

FIGURE 12. (a) First Zagreb vs Entropy (b) Second Zagreb vs Entropy

TABLE 6. Integrity of fit for entropy vs M_1, M_2 indices of Burbankite-type network

Indices	Fit-type	SSE	R^2	$RMSE$
$ENT(M_1)$	$r14$	0.03534	0.9982	0.094
$ENT(M_2)$	$r44$	$1.742e + 08$	0.996	$1.32e + 04$

The first Zagreb index rises quickly at first with increases in entropy, but as entropy increases, its rate of increase slows down, as shown by the plot, exhibiting a logarithmic-like growth. This suggests that the first Zagreb index is extremely responsive in the early phases of growing entropy, capturing the complexity provided by structural changes in the graph as shown in figure 12. The index does, however, saturate at a particular entropy level, suggesting that further complexity or unpredictability in the graph structure has no effect on the initial Zagreb index. The second Zagreb index's saturation implies that it captures increasingly specialised structural characteristics which stabilise as entropy rises. In contrast, more global structural features are captured by the first Zagreb index, which evolves more slowly but still with rising entropy. This implies that although the second Zagreb index is more sensitive to the graph's local connection patterns, the first Zagreb index is more reliable at identifying larger structural alterations. The Numerical Integrity of fit for entropy vs indices of Burbankite-type network are depicted in table 6.

$$ENT(R) = \frac{p_1 x + p_2}{x^5 + q_1 x^4 + q_2 x^3 + q_3 x^2 + q_4 x + q_5}$$

where x is Nbm 119.9 and standard deviation is 104.8. The Coefs (with 95% confidence bounds) are $p_1 = 1.452(0.1209, 2.783)$, $p_2 = 1.578(0.01566, 3.141)$,
$q_1 = 2.658(1.459, 3.857)$, $q_2 = 2.994(-0.1152, 6.102)$, $q_3 = 3.366(-0.7648, 7.497)$, $q_4 = 4.471(-0.0903, 9.031)$, $q_5 = 2.529(0.03437, 5.023)$

$$ENT(H) = \frac{p_1 x + p_2}{x^3 + q_1 x^2 + q_2 x + q_3}$$

where x is Nbm 118.9 and standard deviation is 104.2. The Coefs (with 95% confidence bounds) are $p_1 = 0.8318(-0.1786, 1.842)$, $p_2 = 0.8812(-0.3259, 2.088)$, $q_1 =$

$3.238(1.656, 4.82)$, $q_2 = 4.047(0.3185, 7.776)$, $q_3 = 1.839(-0.442, 4.121)$.

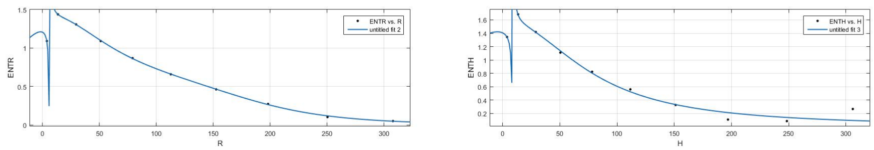

(A) (B)

FIGURE 13. (a) Harmonic Indicaror vs Entropy (b) Randic index vs Entropy

TABLE 7. Integrity of fit for entropy vs R, H indices of Burbankite-type network

Indices	Fit-type	SSE	R^2	$RMSE$
$ENT(R)$	$r15$	0.0004198	0.9994	0.01183
$ENT(H)$	$r13$	0.04443	0.9743	0.09427

The plot in figure 13 shows a decreasing trend, with an increase in entropy leading to a fall in the harmonic index. There appears to be an inverse association as the drop starts out sharply and then slows down as entropy increases. Because of the initial sharp decline, it appears that the harmonic index is especially susceptible to early entropy changes, which indicate substantial alterations in the vertex degree distribution while the graph is still largely ordered. Further increases in entropy have less and less of an effect on the harmonic index as the graph gets more random, causing the index to gradually decline. The Numerical Integrity of fit for entropy vs indices of Burbankite-type network are depicted in table 7.

Plotting indicates that the randić index decreases more quickly than the harmonic index, although it still exhibits a similar declining tendency with entropy. With increasing complexity and disorder on the graph, both the harmonic index and the randić index show a strong inverse connection with entropy, rapidly declining. This suggests that in the early phases of growing entropy, these indices are quite good at capturing structural changes.

$$ENT(\beta_1) = \frac{p_1x^3 + p_2x^2 + p_3x + p_4}{x + q_1}$$

where x is Nbm 8170 and standard deviation is 7601. The coefs (with 95% confidence bounds) are $p_1 = -0.7271(-1.54, 0.08619)$, $p_2 = 0.7748(0.1542, 1.396)$, $p_3 = 2.316(0.9279, 3.704)$, $p_4 = 1.345(0.6374, 2.052)$, $q_1 = 1.064(1.063, 1.064)$

$$ENT(\beta_2) = \frac{p_1x^4 + p_2x^3 + p_3x^2 + p_4x + p_5}{x^2 + q_1x + q_2}$$

where x is Nbm $3.679e+04$ and standard deviation is $3.842e+04$. The coefs (with 95% confidence bounds) are $p_1 = -0.0625(-0.09604, -0.02896)$, $p_2 = 0.0714(0.03204, 0.1108)$, $p_3 = 2.09(2.022, 2.157)$, $p_4 = 3.168(2.97, 3.366)$, $p_5 = 1.253(1.112, 1.394)$, $q_1 = 1.654(1.571, 1.736)$, $q_2 = 0.6792(0.6052, 0.7531)$.

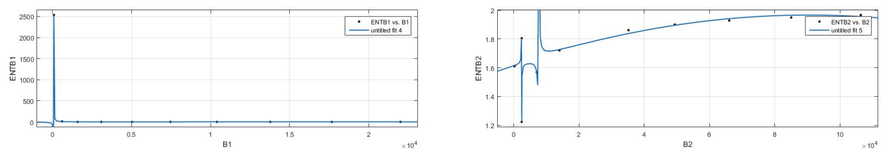

(A) (B)

FIGURE 14. (a) First K Banhatti vs Entropy (b) Second K Banhatti vs Entropy

TABLE 8. Integrity of fit for entropy vs β_1, β_2 indices of Burbankite-type network

Indices	Fit-type	SSE	R^2	$RMSE$
$ENT(\beta_1)$	$r31$	1.368	1	0.5232
$ENT(\beta_2)$	$r42$	0.001156	0.9929	0.01963

Over the reported range, the behaviour of the first K-Banhatti index is almost flat with entropy. This implies that the first K-Banhatti index is not greatly affected by changes in the structural disorder of the graph, indicating that it is rather insensitive to variations in entropy.

The behaviour of the second K-Banhatti index with entropy is more complex, oscillating at lower entropy values before stabilising at higher ones. This suggests that, in low-entropy graphs in particular, the second K-Banhatti index is more sensitive to entropy changes, but that its sensitivity decreases with increasing entropy as shown in figure 14. In the Burbankite-type network, both indices show good fits to entropy; however, the second K-Banhatti index provides a more accurate fit, as seen by the lower RMSE value. Because of this, the second index provides a more precise tool for entropy analysis in this specific type of network shown in table 8.

5. CONCLUSION

We extend the study of the Sombor graph parameter by considering its application to the Burbankite-type network. Furthermore , we explored β_1, β_2, $M_1(G)$, $M_2(G)$, $R(G)$ and $H(G)$ to elaborate Burbankite-Type network and then we execute the general results of these networks.We calculated the entropy based on edge weights for $(Na,Ca)_3(Sr,Ba,Ce)_3(CO_3)_5$ and presented the closed-form expressions for degree-based topological indices along with their corresponding entropy measures. These estimates were compared both numerically and graphically by using MATLAB and Maple

respectively. Curve fitting was performed between various indices and their corresponding entropy values. We evaluated the performance of other MSE-based approaches and found that the rational method consistently yielded the best results, even though the parametric values varied in each case. For entropy versus indices, the rational fit approach produced the best results. Consequently, this research serves as a theoretical tool to better understand how the morphology of
$(Na, Ca)_3(Sr, Ba, Ce)_3(CO_3)_5$ influences its properties, providing guidance for more effective structural modifications in specific applications.

CREDIT AUTHORSHIP CONTRIBUTION'S STATEMENT

All authors contributed equally.

DECLARATIONS

Conflict of Interest: The authors have no conflict of interest.
Funding: All authors funding equally to support this article.
Data Availability: In this article, no data was used.

REFERENCES

[1] Ahmad, A., Koam, A. N., & Azeem, M. (2023). Reverse-degree-based topological indices of fullerene cage networks. *Molecular Physics, 121*(14), 2212-2233.
[2] Ahmad, U., Hameed, S., & Ashfaq, H. A. (2025). Optimizing Cancer Treatment Decisions through Density based-Fuzzy Clustering and Multi-Criteria Decision Making Techniques. *Punjab Univ. j.Math.,57* (11), 1164–1189.
[3] Alikhani, S. & Ghanbari, N. (2021).*Sombor index of polymers.* arXiv preprint arXiv:2103.13663.
[4] Amin, S., Virk, A. U. R., Rehman, M. A., & Shah, N. A. (2021). Analysis of dendrimer generation by Sombor indices. *Journal of Chemistry*, 9930645, 1-15.
[5] Bonchev, D., & Trinajstić, N. (1977). Information theory, distance matrix, and molec-ular branching. *The Journal of Chemical Physics, 67*(10) 4517-4533.
[6] Bonchev, D., Mekenyan, O. V., & Trinajstić, N. (1981). Isomer discrimination by topological information approach. *Journal of Computational Chemistry,2* (2). 127-148.
[7] Bonchev, D., & Rouvray, D. H. (2003). Shannon's information and complexity. In *Complexity in chemistry: Introduction and fundamentals ,7,* 157-187).
[8] Cao, S., & Dehmer, M. (2015). Degree-based entropies of networks revisited. *Applied Mathematics and Computation, 261*, 141-147.
[9] Castellano, G., & Torrens, F. (2015). Information entropy-based classification of triter-penoids and steroids from Ganoderma. *Phytochemistry, 116,* 305-313.
[10] Das, K.C., Çevik, A. S., Cangul, I. N., & Shang, Y. (2021). On Sombor index. S*ymmetry, 13*(1), Article 140.
[11] Das, K.C., Ghalavand, A., & Ashrafi, A. R. (2021). On a conjecture about the Sombor index of graphs. *Symmetry, 13*(10) Article 1830.

[12] Fang, X., You, L., & Liu, H. (2021). The expected values of Sombor indices in random hexagonal chains, phenylene chains and Sombor indices of some chemical graphs. *International Journal of Quantum Chemistry, 121*(17), Article 26740-26760.

[13] N. Ghanbari, & Alikhani, S. (2021). *Sombor index of certain graphs*. arXiv preprint arXiv:2102.10409.

[14] Gutman, I. (2013). Degree-based topological indices. *Croatica Chemica Acta, 86* (4), 351-361.

[15] Gutman, I.(2021). Geometric approach to degree-based topological indices: Sombor indices. *MATCH Communications in Mathematical and in Computer Chemistry, 86* (91), 11-16.

[16] Gutman, I. (2022). TEMO theorem for Sombor index. *Open Journal of Discrete Applied Mathematics, 5*(1), 25-28.

[17] Hayat, S. & Imran, M. (2014). Computation of topological indices of certain networks. *Applied Mathematics and Computation, 240*, 213-228.

[18] S. Hayat, Imran, M., & Liu, J. B. (2019). Correlation between the Estrada index and π-electronic energies for benzene hydrocarbons with applications to boron nanotube. *International Journal of Quantum Chemistry, 119* (23), Article 26016-26030.

[19] Horoldagva, B. & Xu, C. (2023). *On Sombor index of graphs*. arXiv preprint arXiv:2305.04554.

[20] Ibrahim, A. & Gafsa, S. B. (2025). Some new results for reverse graph energies and graph operations. *Punjab Univ. j. Math., 57*(1), 83–105.

[21] Imran, M., Luo, R., Jamil, M. K., Azeem, M., & Fahd, K. M. (2022). Geometric perspective to degree-based topological indices of supramolecular chain. *Results in Engineering, 16,* Article 100716-100730.

[22] Karreman, G. (1955). Topological information content and chemical reactions. B*ulletin of Mathematical Biophysics, 17*, 279-285.

[23] Koam, A.N., Ahmad, A., Asim, M. A., & Azeem, M. (2022). Computation of vertex and edge resolvability of benzenoid tripod structure. *Journal of King Saud University–Science, 34* (6), Article 102-120.

[24] Kulli, V. R. (2016). On K Banhatti indices of graphs. *Journal of Computer and Mathematical Sciences, 7*(4), 213-218.

[25] Liu, H. (2021). *Extremal cacti with respect to Sombor index*. arXiv preprint arXiv:2103.07924.

[26] Liu, H., Chen, H., Xiao, Q., Fang, X., & Tang, Z. (2021). More on Sombor indices of chemical graphs and their applications to the boiling point of benzenoid hydrocar-bons. *International Journal of Quantum Chemistry, 121*(17), Article 26689-26698.

[27] Manzoor, S., Siddiqui, M. K., & Ahmad, S. (2020). On entropy measures of molecular graphs using topological indices. *Arabian Journal of Chemistry, 13*(8), 6285-6298.

[28] W. Ning, , Song, Y., & Wang, K. (2022). More on Sombor index of graphs. *Mathematics, 10*(3), Article 301.

[29] S. OğuzÜnal, (2022). Sombor index over the tensor and Cartesian products of monogenic semigroup graphs. *Symmetry, 14*(5), Article 1071.

[30] J. Rada, , Rodríguez, J. M., & Sigarreta, J. M. (2021). General properties on Sombor indices. *Discrete Applied Mathematics, 299*, 87-97.

[31] Rao,Y., Chen, R., Ahmad, H., & Ahmad, U. (2024). Reverse Zagreb indices and their application in the evaluation of physiochemical properties of anticancer/antibacterial drugs. *ACS Omega, 9*(28), 31056-31080.

[32] Rashchenko, S. V., & Bekker, T. B. (2021). Crystal chemistry of novel "antizeolite" structures. *Journal of Structural Chemistry, 62*(12), 1935-1945.

[33] Refaee, E. A., Ahmad, A., & Azeem, M. (2023). Sombor indices of γ-sheet of boron clusters. *Molecular Physics, 121*(15), Article e2214953.

[34] Sattar, H. S., & Mushtaq, S. (2025). Optimal bounds for the Mostar index of chemical trees. *Punjab Univ. j.Math., 57*(1), 64–84.

[35] Shang, Y. (2022). Sombor index and degree-related properties of simplicial networks. *Applied Mathematics and Computation, 419*, Article 126-146.

[36] Shannon, C. E.(1948). A mathematical theory of communication. *The Bell System Technical Journal, 27*(3), 379-423.

[37] Shannon, C. E. (2001). A mathematical theory of communication. A*CM SIGMOBILE Mobile Computing and Communications Review, 5*(1), 3-55.

[38] Shiba, N. P. , Aremu, K. O., Fatlane, M. J., & Abubakar, M. S. (2026). Reversed degree-based graph invariants in machine learning-driven QSPR analysis of antiviral drugs. *Frontiers in Applied Mathematics and Statistics, 12*, Article 187-198.

[39] Solé, R. V. & Valverde, S. (2004). Information theory of complex networks: On evolution and architectural constraints. In *Complex networks* (pp. 189-207). Springer.

[40] Todeschini, R. & Consonni, V. (2009). *Molecular descriptors for chemoinformatics*. Wiley-VCH.

[41] Youssef, M. Z., Al-Dayel, I., Hanif, M. F., Siddiqui, M. K., Ahmed, H., & Tolasa, F. T.(2024). On statistical evaluation of reverse degree-based topological indices for iron telluride networks. *Scientific Reports, 14*(1), Article 20533-20543.

[42] Zaman , S., Hakami, K. H., Rasheed, S., & Agama, F. T. (2024). Reduced reverse degree-based topological indices of graphyne and graphdiyne nanoribbons with applications in chemical analysis. *Scientific Reports, 14*(1), Article 547-567.

[43] Zhdanov, Y. A. (1979). *Information entropy in organic chemistry*. Rostov University.